The Seismic Velocity Structure of a Traverse Through the Bay of Islands Ophiolite Complex, Newfoundland, an Exposure of Oceanic Crust and Upper Mantle

MATTHEW H. SALISBURY[1] AND NIKOLAS I. CHRISTENSEN

Department of Geological Science and Graduate Program in Geophysics, University of Washington, Seattle, Washington 98195

Although the ophiolites are widely recognized as segments of oceanic crust emplaced on land, direct correlation between the ophiolites and the oceanic crust has proven difficult owing to the near absence of common criteria on which to base a comparison; the ophiolites are defined petrologically, while the oceanic crust is defined largely in terms of seismic structure. To bridge this gap the seismic velocity structure of a traverse through the Blow-Me-Down massif of the Bay of Islands ophiolite complex, Newfoundland, has been reconstructed in detail from values of compressional (V_p) and shear (V_s) wave velocity measured in the laboratory under conditions of hydrostatic confining pressure and water saturation thought to approximate conditions in the oceanic crust through oriented samples collected from 60 closely spaced sites of known stratigraphic level. The velocity structure thus determined is indistinguishable from that of normal oceanic crust: The uppermost velocity unit in the massif consists of 0.5 km of prehnite-pumpellyite facies metabasalt with $V_p \leq 5.70$ and $V_s \leq 3.10$ km/s, underlain by 0.8 km of greenschist facies pillow basalts and brecciated dikes with $V_p \leq 6.20$ and $V_s \leq 3.35$ km/s. Between 1.3 and 6.4 km, in a thick unit composed of metadolerite sheeted dikes underlain by coarse-grained metagabbro grading downward through pyroxene and troctolitic olivine gabbro, V_p and V_s increase from 6.75 and 3.75 km/s near the top to 7.40 and 3.90 km/s near the base, respectively. This increase is gradational, except at 5.3 km, where a step increase in V_p to 7.40 km/s marks an increase in olivine content. A sharp velocity inversion in V_p, caused by quartz-rich late differentiates, is found in the upper levels of this unit between 2.8 and 3.3 km. The deepest level of the complex, composed of ultramafics, is characterized by values of V_p and V_s of 8.4 and 4.9 km/s, respectively. A comparison of the seismic velocity structure and petrology of the traverse across the Blow-Me-Down massif with oceanic seismic structure suggests that at many sites in the ocean basins, (1) layer 2 consists of prehnite-pumpellyite and greenschist facies pillow basalts and brecciated dikes, (2) the layer 2-3 boundary separates greenschist facies metabasalts and brecciated dikes at the base of layer 2 from epidote-amphibolite facies sheeted dikes at the top of layer 3, (3) layer 3 consists of metadolerite sheeted dikes underlain by metagabbro, pyroxene gabbro, and troctolitic olivine gabbro, (4) the 7.4-km/s basal layer observed in sonobuoy studies consists of interlayered olivine gabbro, troctolite, and plagioclase peridotite, (5) the Mohorovičić discontinuity represents a relatively sharp transition from gabbro to dunite and peridotite, and (6) pronounced, but laterally discontinuous, velocity inversions may be present at the base of layer 2 below the relatively high velocity prehnite-pumpellyite facies metabasalt level and at intermediate levels in layer 3 in association with late differentiates.

INTRODUCTION

Although the ophiolites are widely regarded as fragments of oceanic crust tectonically emplaced on land, direct correlation between the ophiolites and the oceanic crust remains difficult owing to the near absence of common grounds for comparison: the ophiolites are defined largely in terms of petrologic and structural field relations, whereas the majority of the oceanic crust, owing to its inaccessibility, is best defined in geophysical terms, specifically, its velocity structure as revealed by seismic refraction. To evaluate the ophiolite hypothesis thus requires either a detailed knowledge of the petrology of the oceanic crust as a function of depth or detailed knowledge of the velocity structure of the ophiolites.

With the exception of samples recovered from the uppermost levels of layer 2 by drilling, the petrology of the oceanic crust is known only from dredge samples of uncertain tectonic provenance and stratigraphic level. Though the petrology of such samples [e.g., *Engel and Fisher,* 1969; *Miyashiro et al.,* 1971] is, in many instances, strikingly similar to that of the ophiolites [e.g., *Gass and Masson-Smith,* 1963; *Davies,* 1971; *Church and Stevens,* 1971; *Moores and Vine,* 1971; *Varne and Rubenach,* 1972; *Gass and Smewing,* 1973] and their velocities are consistent with oceanic refraction velocities [*Fox et al.,* 1973], direct correlation is precluded until the igneous stratigraphy of the oceanic crust has been determined through deep basement drilling.

Attempts to determine the velocity structure of the ophiolites through on-land refraction studies through major ophiolite complexes have been similarly unsuccessful. In situ velocities measured in the Troodos complex [*Matthews et al.,* 1971; *Lort and Matthews,* 1972], for example, are invariably low in comparison to velocities observed at sea. This discrepancy can be ascribed to five mechanisms, initiated, presumably, by emplacement of such complexes on land: (1) subaerial weathering, (2) a decrease in hydrostatic confining pressure at all levels due to the erosional removal of the upper levels of the complex, (3) the draining of water from pores, joints, and fractures following subaerial exposure and lowering of the water table, (4) the introduction of new joints and fractures by unloading and the emplacement mechanism itself, and (5) partial to pervasive serpentinization in the ultramafics. That each of these mechanisms strongly lowers seismic velocity, particularly within the range of pressures relevant to the oceanic crust (0–3 kbar), is well established [*Birch,* 1960; *Christensen,* 1966; *Nur and Simmons,* 1969; *Dortman and Magid,* 1969; *Christensen and Salisbury,* 1972, 1973]. Changes of velocity caused by these mechanisms are so variable, however, that correction of the data for these effects has proven infeasible.

[1] Now at Scripps Institution of Oceanography, University of California, La Jolla, California 92093.

Paper number 7B0970.
0148-0227/78/027B-0970$03.00

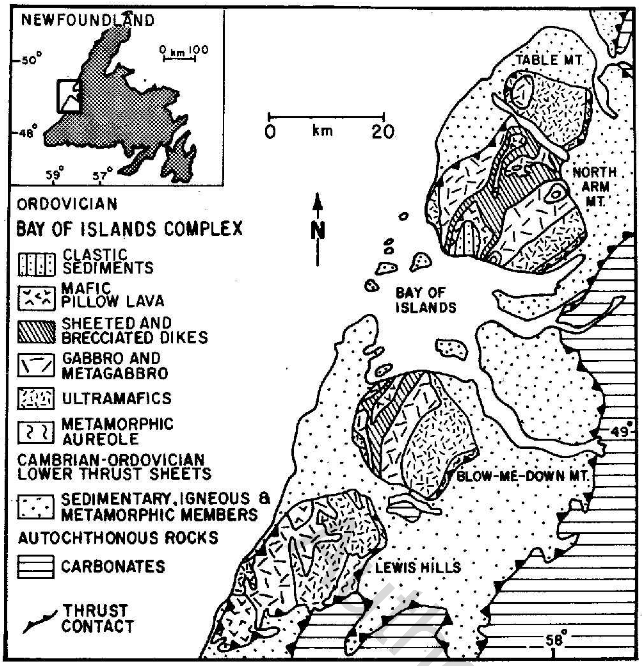

Fig. 1. Geology of the Bay of Islands complex, Newfoundland [after *Williams*, 1971].

Although the velocity structures of ophiolites cannot be determined directly from field measurements, they can be reconstructed in the laboratory. Preliminary studies of velocity through samples recovered from ophiolites [*Dewey et al.*, 1973; *Poster*, 1973; *Peterson et al.*, 1974; *Christensen*, 1975] have confirmed that rocks of the ophiolite suite display velocities roughly similar to those commonly observed in oceanic refraction studies. The purpose of the present investigation is to reconstruct, by means of laboratory measurements of velocity through oriented samples of known geologic context and stratigraphic level, a detailed velocity column through a major ophiolite complex and to compare this column with the observed velocity structure of the oceanic crust and upper mantle.

Of the several hundred ophiolites cited in the literature, the Bay of Islands complex was selected for this study for the following reasons: (1) Most ophiolites are so sheared and dismembered by faulting that major petrologic levels are partially or entirely missing. The Bay of Islands complex is unusual, however, in that it appears to be petrologically complete and relatively uncomplicated in selected areas, allowing accurate stratigraphic reconstruction. (2) There is little evidence in the complex of metamorphism associated with post-emplacement tectonic events. (3) Most exposures display only minimal weathering. Deeply weathered surficial levels have been removed by late Pleistocene glaciation. (4) The presence

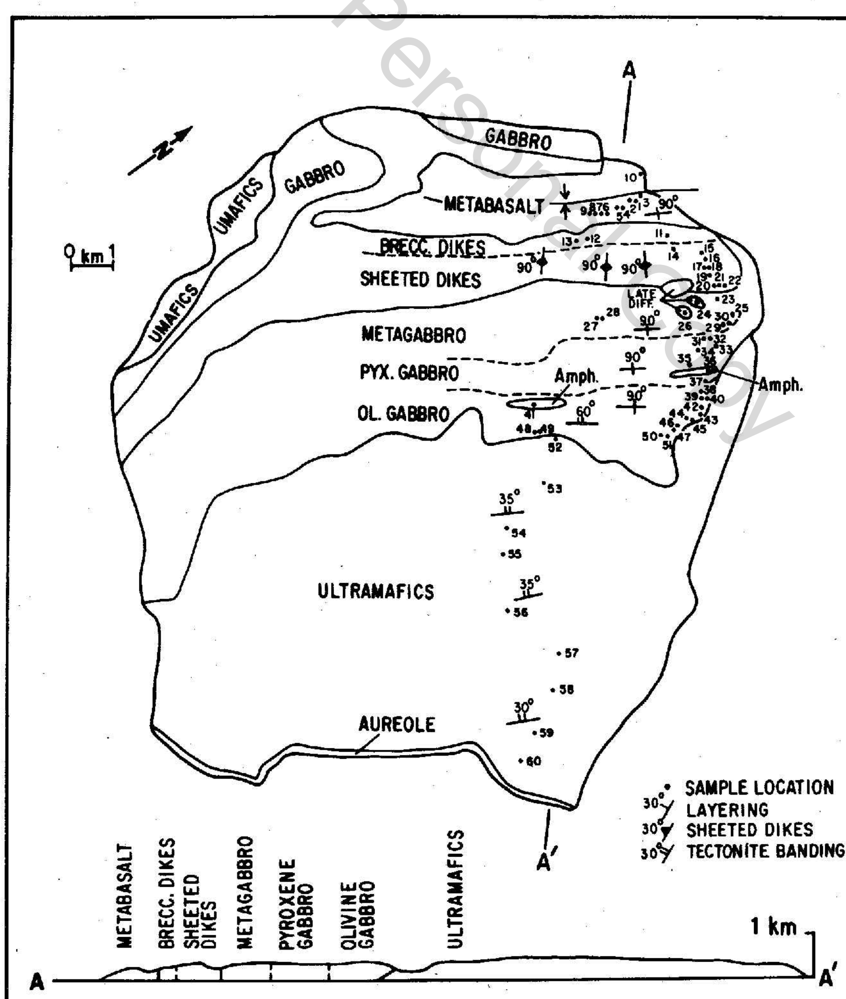

Fig. 2. Geology of the Blow-Me-Down massif, Bay of Islands complex, showing sample locations and representative values of strike and dip.

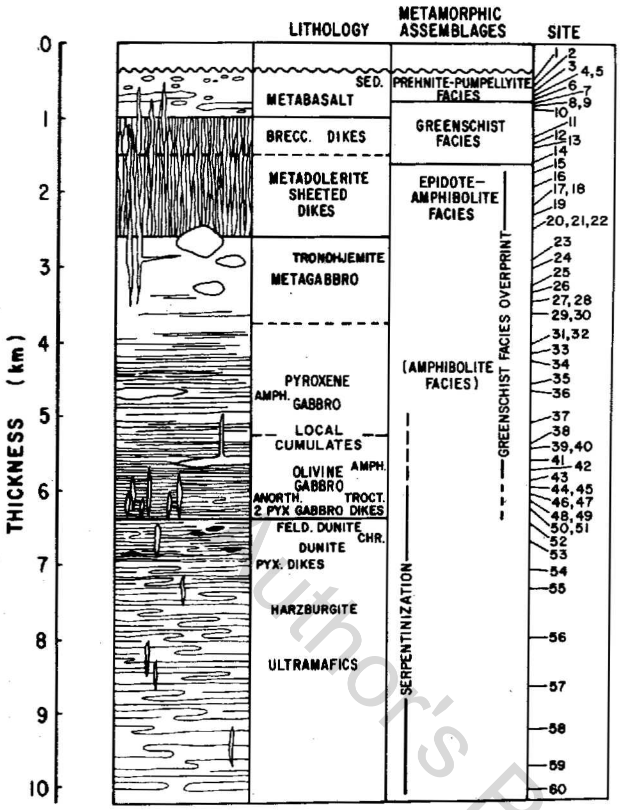

Fig. 3. Stratigraphy of the Blow-Me-Down massif, Bay of Islands complex.

of sheeted dikes and local cumulate layering in the complex provides a structural reference frame for the collection of oriented samples for the study of seismic anisotropy patterns and the comparison of such patterns with those observed in oceanic refraction data. (5) The Bay of Islands complex has excellent exposures at nearly all structural levels, is reasonably accessible, and has been mapped at least in reconnaissance fashion throughout [*Smith,* 1958; *Williams,* 1971].

Through extensive collection of fresh, oriented samples from all levels of the complex and subsequent laboratory studies, it has been possible to reconstruct the compressional (V_p) and shear (V_s) wave velocity columns for a traverse across the Bay of Islands ophiolite complex in considerable detail, to construct from these the Poisson's ratio (σ) column for the traverse, and to relate both the general configuration of these columns and the specific features, such as velocity gradients and inversions, to changes in petrology and density with depth. Finally, it has been possible to evaluate the ophiolite hypothesis through a comparison of these data with the seismic structure of the oceanic crust.

GEOLOGY OF THE BLOW-ME-DOWN MASSIF OF THE BAY OF ISLANDS OPHIOLITE COMPLEX

The Bay of Islands ophiolite complex, located on the western coastline of Newfoundland, consists of four isolated, plateaulike massifs totaling approximately 750 km² in area (Figure 1). The complex is considered to represent a once continuous thrust sheet of Lower Ordovician oceanic crust and upper mantle emplaced as the uppermost of a series of thrust sheets from the east during the Middle Ordovician [*Williams et al.,* 1972]. Only the uppermost thrust is considered an ophiolite; lower levels consist largely of clastic carbonate deposits thrust over shallow water carbonates and flysch deposited unconformably on crystalline basement rocks of Grenville age [*Williams,* 1973]. Ranging from the top downward in the uppermost thrust are found lithified clastic sediments, pillow basalts with intercalated sediments and flows, a sheeted dike complex, and a thick sequence of gabbros. Small intrusive bodies of diorite, trondhjemite, and olivine gabbro are common at the level immediately below the sheeted dikes; pyroxenite and anorthosite dikes are found at the base of the gabbroic section. Underlying the gabbros are ultramafics composed of dunite, peridotite, pyroxenite, and podiform chromitite. Finally, the deepest levels of the complex are composed solely of peridotite. The basal contact with the underlying sediments is marked along the eastern margin by a high-temperature metamorphic aureole of garnet amphibolite [*Williams and Smyth,* 1973].

Though the four massifs shown in Figure 1 display strong similarities, two are incomplete (Lewis Hills and Table Mountain), and a third (North Arm Mountain) is complicated by faults and second-order folding. Preliminary mapping suggests, however, that Blow-Me-Down Mountain is both structurally uncomplicated over large areas and stratigraphically complete, or nearly so; of the lithologies cited above, only the sedimentary unit and the uppermost levels of the basalt are missing, both having been removed by erosion. Since on the basis of structure and petrology the Blow-Me-Down massif is most suited to the objectives of this study, only this portion of the complex will be considered further.

Within the section selected for velocity measurements (Figure 2), bedding, indicated at extrusive levels by intercalated sediments and flow surfaces and at plutonic levels by local cumulate layering, has an average strike of N35°E and dips vertically, with up lying to the northwest. In the vicinity of the gabbro-ultramafic contact the layering gradually assumes a 35° dip to the northwest, an attitude maintained throughout the remaining ultramafic levels. Both the sheeted dikes and the isolated dikes shown at deeper levels in Figure 2 display a remarkably constant subvertical orientation with an average strike of N50°W. This orientation is roughly perpendicular to bedding at all levels. This relative structural simplicity and the presence of either sedimentary or igneous layering at most levels allow the stratigraphy of the massif to be reconstructed as described below and summarized in Figure 3 for a traverse along the line A-A′ shown in Figure 2.

0–1.0 km—Pillow basalts. The uppermost unit exposed in the Blow-Me-Down massif consists of approximately 0.6 km of metabasalts with preserved pillow and flow structures and minor intercalated red cherts from which, through comparison with exposures on the North Arm massif, it is estimated that an additional 0.4 km of basalt and an unknown thickness of sediments have been stripped by erosion. In the uppermost 0.3 km (the 0.4- to 0.7-km level, referred to the estimated top of the extrusives) the metabasalts are typically fine grained with hypidiomorphic, intersertal, or subvariolitic textures and a highly altered groundmass. Relic clinopyroxene is commonly present, and plagioclase is usually albite in composition. Pumpellyite occurs as radiating clusters and patches within the groundmass and as rims within amygdules. Sphene, chlorite, hematite, and quartz are present in the groundmass. Calcite-filled veins and amygdules are common. Below this level, between 0.7 and 1.0 km, the basalts have been pervasively metamorphosed to greenschist facies assemblages, the groundmass and phenocrysts being almost entirely replaced by chlorite, actinolite, epidote, and albite.

Dikes of irregular orientation are common, particularly near the base of the unit. The dikes tend to be fine grained and subophitic in texture. Mineralization arising from hydrothermal activity occurs as small deposits of pyrite, chalcopyrite, pyrrhotite, and traces of native copper in the vicinity of late stage dikes.

1.0–1.5 km—Brecciated dikes. Immediately below the pillow lavas and transitional between them and an underlying sheeted dike complex is found a dense to sheeted swarm of brecciated dikes approximately 0.5 km in thickness, which is now largely healed by metamorphism. The brecciation, ranging from microscopic to hand sample in scale and extending over broad areas at or near this stratigraphic level, does not appear to be tectonic in origin but rather to have formed by gas fluidization caused by the contact of seawater with hot dike material under conditions of high confining pressure [*Williams and Malpas,* 1972]. The upper and lower limits of the unit are not sharp but statistical in nature, being best described as irregular boundaries within which brecciated dikes predominate over basalts and unbrecciated sheeted dikes, respectively. Compositionally and texturally, the brecciated dikes consist of fine-grained metadolerite with greenschist facies mineral assemblages similar to those found in the lower levels of the pillow basalts.

1.5–2.6 km—Sheeted dikes. Underlying and feeding upward into the brecciated dikes, as well as being intruded by them, is a well-developed complex of sheeted dikes, approximately 1.1 km thick, composed of subvertical intrusive dikes averaging 0.5 m in width, each emplaced against the next, with no country rock. The dikes are for the most part one-sided, with chill margins predominately to the southwest. A small number of dikes, constituting perhaps 10% of the unit, are sulfide rich, pale in color, and two-sided, suggesting emplacement during late-stage intrusive activity.

The upper 0.1 km of the sheeted dikes contains greenschist facies mineral assemblages, but below this level, epidote-amphibolite mineral assemblages predominate; green hornblende becomes the abundant amphibole, mosaic recrystallization aggregates of oligoclase-andesine are common, and epidote is present as intergrowths with hornblende. Of significance, greenschist facies mineral assemblages are also locally present within the lower levels of the sheeted dikes. Minerals include actinolite, albite, chlorite, and epidote formed by saussuritization of plagioclase. Textural relations clearly show that these minerals have formed after epidote-amphibolite assemblages. Traces of relic pyroxene and plagioclase with a subophitic texture indicate that the original dike rocks were dolerites.

2.6–3.8 km—Metagabbros and late differentiates. Below the sheeted dikes the massif changes abruptly to a 1.2-km-thick unit of relatively coarse-grained metagabbro cut by small intrusive bodies of diorite and trondhjemite. The metagabbros are rich in green hornblende, epidote, and oligoclase-andesine and, unlike the sheeted dikes above, commonly contain relic clinopyroxene. When it is found in layered rocks, the clinopyroxene tends to be intercumulus with cumulus plagioclase. Small amounts of olivine and primary brown hornblende are also present, the latter as rims around pyroxene. As in the sheeted dikes, greenschist facies metamorphism has overprinted the epidote-amphibolite facies metamorphism; the plagioclase is often saussuritized, hornblende and clinopyroxene are replaced by intergrowths of actinolite-tremolite, anhedral quartz patches are common, and intergranular and vein chlorite is present. The trondhjemites and diorites found at this level appear to be late differentiates from underlying cumulates.

3.8–5.3 km—Pyroxene gabbros. Between depths of 3.8 and 5.3 km the massif is composed predominantly of pyroxene gabbro with subordinate amounts of anorthositic olivine gabbro, hornblende gabbro, and amphibolite. Cumulate layering is locally developed toward the base of the subunit where cyclic, 'inch scale' phase layering is observed. Plagioclase is often moderately to strongly aligned with long axes subparallel to layering. Recrystallization patches and veins of tremolite-actinolite, epidote, albite, and chlorite are locally abundant. Hornblende and epidote clusters are also common. Olivine gabbros are present but uncommon at this level. What little olivine was initially present has been largely replaced by serpentine.

Toward the base of the unit are found small pods of fine-grained amphibolite displaying protoclastic or cataclastic texture and strong foliation parallel to layering. That the texture is intrusive rather than cataclastic is suggested by the presence nearby of small feeder dikes of similar material displaying foliation perpendicular to layering and parallel to the dike walls. If, however, the texture is cataclastic and the pods represent mylonite zones, the displacement is small, since the lithology is unchanged across the fault.

5.3–6.4 km—Basal olivine gabbros and troctolites. The deepest level of the gabbros is a complex interlayered zone composed of tectonized anorthositic olivine gabbro, troctolite, and plagioclase peridotite. The scale of banding is quite variable but generally increases downward from a few centimeters per layer near the top to tens of meters near the base. The plagioclase tends to be strongly aligned and is frequently altered to epidote along cleavage and fractures. Olivine is partially replaced by actinolite, talc, chlorite, and serpentine. Augite and primary brown hornblende are ubiquitous as minor constituents, while enstatite is rare.

Instrusives are common between 5.5 and 5.7 km as sills and small dikes of fine-grained amphibolite intruding olivine gabbro. As at higher levels, the amphibolites are strongly foliated parallel to layering but display, in addition, a strong lineation locally perpendicular to the plane of the sheeted dikes. Near the base of the gabbros and totaling perhaps 20% of the outcrop in the vicinity of the contact with the underlying ultramafics, are found numerous two-sided dikes and sills of two-pyroxene gabbro containing hypersthene and augite (often with hornblende and minor secondary actinolite) and occasional dikes of anorthosite, the latter displaying strong alignment of plagioclase long axes parallel to the plane of the sheeted dikes.

6.4–10.8 km—Ultramafics. At the base of the gabbros, in a strongly banded, locally mylonitic transition zone less than 50 m thick composed of partially serpentinized feldspathic dunite in which olivine increases downward at the expense of plagioclase, the massif changes rapidly to an ultramafic composition. For 0.6 km below this transition zone, the ultramafics are tectonized and composed predominantly of serpentinized dunite with minor amounts of banded and podiform chromitite, partially serpentinized harzburgite, and small dikes of pegmatitic clinopyroxenite.

The deepest levels exposed in the massif are thick units of ultramafic tectonites composed of partially serpentinized harzburgite and dunite. The tectonites are strongly banded at intermediate levels, the bands consisting of gently to isoclinally folded layers of harzburgite, alternately rich in olivine and enstatite, between 0.02 and 1.0 m thick. The banding shows no evidence (such as cyclic layering or graded bedding) of being cumulate in origin. At intermediate and deep levels, relic enstatite is commonly found in association with minor clinopyroxene, while spinels are found at all levels.

As was noted earlier, the Bay of Islands complex is juxta-

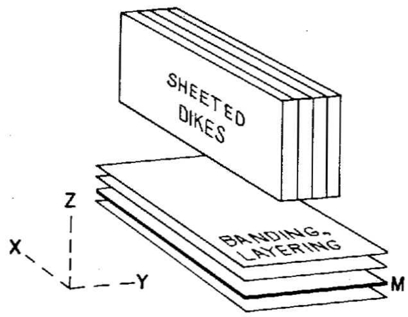

Fig. 4. Core orientation criteria.

posed against country rock along a thrust fault at its base. The fault is variable in nature throughout the complex, but under the ultramafics it appears to be thermally annealed, with flaser textures just above the fault and a garnet amphibolite metamorphic aureole, retrograde downward, imprinted below, suggesting emplacement of the complex while still at elevated temperatures.

Though strikingly similar to continental layered intrusions, and in fact mistaken for one by early writers [e.g., *Buddington and Hess,* 1937; *Smith,* 1958], the Bay of Islands complex nonetheless differs petrologically from these bodies in that most levels have been profoundly influenced by water. Judging from the presence of primary hornblende throughout the intrusive levels, it is apparent that the magma itself either contained small amounts of juvenile water or was contaminated by seawater. Metamorphism, which increases in grade downward from prehnite-pumpellyite, to greenschist, and finally to epidote-amphibolite facies with a weak greenschist facies overprint, dominates the mineralogy of the upper levels of the complex. Since this metamorphism increases in grade but decreases in intensity with depth and is confined to the vicinity of dikes in the lower gabbros, it appears to be related to deep penetration of seawater along joints and fractures followed by retrograde metamorphism, perhaps as the crust was carried away from the ridge, rather than to postemplacement metamorphism. Finally, it should be noted that the basal gabbros and troctolites and the underlying ultramafics have been partially serpentinized, apparently by meteoric water [*Wenner and Taylor,* 1973], either during or after emplacement on land.

PROCEDURES AND DATA

Beginning in the summer of 1973 an extensive program of sampling for laboratory studies was undertaken on the Blow-Me-Down massif of the Bay of Islands complex. Although site selection was to a certain extent dictated by the availability of outcrop, it was possible, as can be seen from the site locations shown in Figure 2, to collect specimens at closely spaced intervals from all stratigraphic levels of the massif within a relatively narrow band extending downsection to the base of the complex. At each of the 60 sites sampled, care was taken to obtain large, fresh, and, in the ultramafics, minimally serpentinized specimens suitable for coring. In addition, at 32, or more than half, of the sites, oriented samples were taken for anisotropy studies, and 94 strike and dip measurements, of which representative examples are shown in Figure 2, were taken on such features as bedding, cumulate layering, tectonite banding, foliation, and dike and sill orientation to allow detailed structural and stratigraphic reconstruction.

Once in the laboratory, cylindrical cores were obtained from each sample by using a 1.25-, 1.90-, or 2.54-cm diamond bit, the diameter being selected on the basis of grain size. Each core was trimmed and polished to a right cylinder approximately 3 times its diameter in length, with ends parallel to within 0.5°. After drying, the bulk density of each core was determined from its mass and measured dimensions. Wherever possible, three mutually perpendicular cores, designated cores 1, 2, and 3, were taken from each sample to check for homogeneity and seismic anisotropy. In the case of field-oriented samples, cores were taken parallel to each of the three orthogonal coordinates indicated in Figure 4; one core, designated $1x$, was taken with its long axis simultaneously parallel to the plane of the sheeted dikes and to the regional layering plane, while a second, $2y$, was cored perpendicular to the sheeted dikes and $3z$ was cored perpendicular to layering. It should be noted in Figure 4 that the layering was assumed to have been initially horizontal. The orientation of cores 1 and 3 and the estimated layer thicknesses will be in error to the extent that this assumption is incorrect.

Prior to the actual measurement of velocity through each sample, the cores were immersed in water for a minimum of 48 hours, to allow the samples to become water saturated. Each core was then jacketed in thin copper foil and gum rubber tubing to prevent the pressure medium from penetrating the sample at high pressure. Where high sample porosities were anticipated, as in the extrusives and sheeted dikes, 100-mesh screen was placed between the core and the jacket to provide void space into which pore water from the sample could drain during compression. By this means, pore pressure was maintained much lower than confining pressure.

Velocities were measured in all samples at room temperature with both rising and descending pressure at 0.2-kbar intervals for confining pressures between 0 and 1.0 kbar, at 0.5-kbar intervals between 1.0 and 2.0 kbar, and at 1.0-kbar intervals between 2.0 and 6.0 kbar by using the pulse transmission technique described by *Birch* [1960] and *Christensen and Shaw* [1970]. Compressional and shear waves were generated across each sample by means of barium titanate and ac-cut quartz transducers, respectively, having resonant frequencies of 2 MHz. The cumulative error limits for compressional and shear wave velocities are estimated to be 0.5% and 1.0%, respectively. Confining pressures, measured by means of a manganin coil exposed directly to the pressure medium, are considered accurate to within 1%.

Compressional and shear wave velocity data, together with computed values, corrected for length change, of Poisson's ratio σ, are presented at calculated in situ confining pressures in Table 1 for 46 sites from the Blow-Me-Down massif of the Bay of Islands complex. Also presented for each sample are values of measured and mean bulk density ρ and the stratigraphic level at which the sample was recovered. In addition, reconstructed compressional and shear wave velocities are shown for partially serpentinized samples from 14 sites in the lower levels of the massif. These have been reconstructed from estimates of the original modal composition based on thin section analysis and a linear interpolation of velocity between olivine, enstatite, augite, and plagioclase end-members having compressional and shear wave velocities determined from isotropic samples at 2.5 kbar of 8.46 and 4.92, 7.89 and 4.76, 7.58 and 4.37, and 6.99 and 3.55 km/s, respectively. It should be noted that neither linear interpolation nor the velocities cited are likely to be rigorously correct over the entire range of conditions under consideration. Since the velocities reported are thus only approximate (±0.1 km/s), no attempt has been made to compute values of Poisson's ratio σ for these samples. A more sophisticated treatment of the ultramafics, taking into account the effects of anisotropy, will be presented in a later study.

TABLE 1. Compressional (P) and Shear (S) Wave Velocities for Samples From the Blow-Me-Down Massif at Confining Pressures (P_C) Appropriate to the Sea Floor

Site	Lithology	Depth, km	P_C, kbar	Density, g/cm³ 1	2	3	Mean	Velocity, km/s Mode	1	2	3	Mean	Poisson's Ratio
1	Metabasalt	0.48	0.6	2.72	2.71		2.72	P	*5.79*	5.67		5.73	0.30
								S	*3.07*				
2	Metabasalt	0.50	0.6	2.73	2.74		2.73	P	5.50 x	*5.72 y*		5.61	0.31
								S		*3.00 y*			
3	Metabasalt	0.55	0.7	2.75	2.78		2.77	P	*6.06*	6.05		6.05	0.28
								S	*3.37*				
4	Metabasalt	0.58	0.7	2.89	2.80		2.84	P	*6.17*	6.13		6.15	0.22
								S	*3.69*				
5	Metabasalt	0.58	0.7	2.84	2.85		2.85	P	*6.22*	6.14		6.18	0.29
								S	*3.39*				
6	Metabasalt	0.67	0.7	2.84	2.82		2.83	P	6.38 x	*6.34 y*		6.36	0.29
								S		*3.46 y*			
7	Metabasalt	0.70	0.7	2.81	2.85		2.83	P	6.29 x	*6.31 y*		6.30	0.30
								S		*3.40 y*			
8	Metabasalt	0.73	0.7	2.86	2.87		2.86	P	6.20 x	*6.19 y*		6.20	0.28
								S		*3.40 y*			
9	Metabasalt	0.73	0.7	2.84				P	*6.05*				0.29
								S	*3.29*				
10	Metabasalt	0.82	0.7	2.88	2.88	2.86	2.87	P	6.14	6.22	6.25	*6.20*	0.31
								S	3.24	3.30	3.29	*3.28*	
11	Metadolerite	1.27	0.9	2.84				P	*6.20*				0.30
								S	*3.31*				
12	Metadolerite	1.34	0.9	2.93				P	*6.58*				0.28
								S	*3.62*				
13	Metadolerite	1.37	0.9	2.90	2.88		2.89	P	6.43 x	*6.36 y*		6.40	0.29
								S		*3.46 y*			
14	Metadolerite	1.53	0.9	2.84	2.83	2.83	2.83	P	6.52 x	6.47 y	6.49 z	6.49	0.29
								S		*3.52 y*			
15	Metadolerite	1.65	1.0	2.92	2.90	2.92	2.91	P	6.64 x	*6.76 y*	6.75 z	6.72	0.28
								S		*3.75 y*			
16	Metadolerite	1.85	1.0	2.93	2.95	2.94	2.94	P	6.70 x	*6.78 y*	6.77 z	6.75	0.27
								S		*3.78 y*			
17	Metadolerite	2.05	1.1	2.91	2.88	2.88	2.89	P	6.72	7.04	6.75	*6.84*	0.28
								S	3.81	3.86	3.75	*3.81*	
18	Metadolerite	2.05	1.1	2.86	2.83	2.84	2.84	P	*6.70*	6.80	6.78	6.76	0.26
								S	*3.80*				
19	Metadolerite	2.20	1.1	2.93				P	*6.79*				0.28
								S	*3.77*				
20	Metadolerite	2.48	1.2	2.96	2.95		2.95	P	6.74 x	*6.69 y*		6.71	0.27
								S		*3.74 y*			
21	Metadolerite	2.48	1.2	2.92	2.92	2.94	2.93	P	6.76	6.72	6.70	*6.73*	0.27
								S	3.76	3.80	3.77	*3.78*	
22	Metadolerite	2.48	1.2	2.88	2.87	2.89	2.88	P	*6.70*	6.63	6.75	6.69	0.27
								S	*3.75*				
23	Metagabbro	2.85	1.3	2.90				P	*6.74*				0.26
								S	*3.85*				
24	Trondhjemite	2.92	1.3	2.57	2.57		2.57	P	6.07	*6.06*		6.07	0.24
								S		*3.57*			
25	Metagabbro	3.28	1.4	2.96	2.91	2.88	2.92	P	6.70 x	*6.73 y*	6.77 z	6.73	0.28
								S		*3.70 y*			
26	Metagabbro	3.34	1.5	2.82	2.80		2.81	P	6.28 x	*6.31 y*		6.30	0.28
								S		*3.49 y*			
27	Metagabbro	3.45	1.5	2.91	2.90		2.90	P	6.59 x	*6.62 y*		6.60	0.28
								S		*3.63 y*			
28	Metagabbro	3.45	1.5	2.93	2.94		2.93	P	*6.83 x*	6.97		6.90	0.27
								S	*3.86 x*				
29	Metagabbro	3.65	1.5	2.88	2.92	2.94	2.91	P	6.66	6.48	*6.58*	6.57	0.28
								S			*3.65*		
30	Metagabbro	3.65	1.5	2.97	2.92		2.95	P	6.66	6.46		*6.56*	0.28
								S	3.62	3.67		*3.64*	
31	Metagabbro	3.97	1.6	2.90	2.91	2.91	2.91	P	7.04 x	*7.00 y*	7.12 z	7.06	0.29
								S		*3.82 yz*			
32	Metagabbro	3.97	1.6	2.90	2.89	2.87	2.89	P	7.04 x	*6.89 y*	7.01 z	6.98	0.27
								S		*3.88 yz*			
33	Gabbro	4.14	1.7	2.84	2.88	2.86	2.86	P	7.01	6.86	6.94	*6.94*	0.30
								S	3.61	3.70	3.75	*3.69*	
34	Gabbro	4.30	1.7	2.84	2.83		2.83	P	7.01 x	*7.09 y*		7.05	0.29
								S		*3.84 yz*			
35	Gabbro	4.78	1.9	2.90	2.90	2.85	2.88	P	6.87 x	*6.90 y*	7.09 z	6.95	0.30
								S		*3.70 yz*			
36	Amphibolite	4.86	1.9	2.94	2.98	2.97	2.96	P	7.20 x	*7.10 y*	6.88 z	7.06	0.27
								S		*3.96 yz*			

TABLE 1. (continued)

Site	Lithology	Depth, km	P_C, kbar	Density, g/cm³ 1	2	3	Mean	Mode	Velocity, km/s 1	2	3	Mean	Poisson's Ratio
37	Metagabbro	5.08	1.9	2.80	2.84	2.80	2.81	*P*	6.81 *x*	*6.88 y*	7.07 *z*	6.92	0.29
								S		*3.75 yz*			
38	Olivine gabbro	5.37	2.0	2.95	2.96	2.96	2.95	*P*	7.12 *x*	*7.15 y*	7.29 *z*	7.19	0.29
								S		*3.90 yz*			
39	Olivine gabbro	5.44	2.0	2.94	2.96	2.94	2.95	*P*	*7.18 x*	7.12 *y*	7.32 *z*	7.21	0.32
								S	*3.72 xz*				
40	Olivine gabbro	5.44	2.0				(3.3)	*P*				(8.25)	
								S				(4.75)	
41	Amphibolite	5.64	2.1	3.02	3.00		3.01	*P*	7.29 *x*	*7.46 y*		7.38	0.30
								S		*3.98 yz*			
42	Olivine gabbro	5.75	2.1	2.99	2.98	2.98	2.98	*P*	7.31 *x*	*7.27 y*	7.17 *z*	7.25	0.31
								S		*3.85 yz*			
43	Troctolite	5.92	2.2				(3.3)	*P*				(7.30)	
								S				(3.85)	
44	Olivine gabbro	6.00	2.2				(3.3)	*P*				(7.35)	
								S				(3.90)	
45	Anorthosite	6.00	2.2	2.74	2.73		2.73	*P*	6.96	*7.17 y*		7.07	0.31
								S		*3.77 y*			
46	Olivine gabbro	6.12	2.2				(3.3)	*P*				(7.30)	
								S				(3.85)	
47	Gabbro	6.13	2.2	2.97	2.94		2.96	*P*	*6.95*	6.99		6.97	0.28
								S	*3.83*				
48	Troctolite	6.22	2.3				(3.3)	*P*				(7.30)	
								S				(3.85)	
49	Troctolite	6.22	2.3				(3.3)	*P*				(7.95)	
								S				(4.45)	
50	Gabbro	6.23	2.3	3.03	3.02	2.99	3.01	*P*	6.88	*6.92*	6.98	6.93	0.27
								S		*3.89*			
51	Gabbro	6.23	2.3	3.00	2.95	2.99	2.98	*P*	6.96 *x*	*6.94 y*	7.10 *z*	7.00	0.29
								S		*3.75 yz*			
52	Feldspathic dunite	6.41	2.3				(3.3)	*P*				(8.25)	
								S				(4.70)	
53	Pyroxenite	6.70	2.4	3.23				*P*	*7.64*				0.25
								S	*4.43*				
54	Harzburgite	7.02	2.5				(3.3)	*P*				(8.40)	
								S				(4.90)	
55	Dunite	7.31	2.6				(3.3)	*P*				(8.45)	
								S				(4.90)	
56	Dunite	7.99	2.8				(3.3)	*P*				(8.45)	
								S				(4.90)	
57	Harzburgite	8.70	3.1				(3.3)	*P*				(8.30)	
								S				(4.85)	
58	Harzburgite	9.21	3.2				(3.3)	*P*				(8.40)	
								S				(4.90)	
59	Harzburgite	9.77	3.4				(3.3)	*P*				(8.30)	
								S				(4.90)	
60	Harzburgite	10.8	3.5				(3.3)	*P*				(8.35)	
								S				(4.90)	

Here 1, 2, 3 and *x*, *y*, *z* are core orientation criteria; see Figure 4 and text for explanation. Values in italics are used in the computation of Poisson's ratio. Values in parentheses indicate that the sample was serpentinized and the values reconstructed from modal analysis, an isotropic aggregate being assumed.

The measured velocities reported in Table 1 were determined from the curves of measured velocity versus confining pressure discussed above and in situ confining pressures calculated from the relation,

$$P_c = (\rho g z' \times 10^{-9}) + 0.5$$

where P_c is the hydrostatic confining pressure in kilobars at the stratigraphic level under consideration, ρ is the average density of the overlying rock column in grams per cubic centimeter, g is the acceleration of gravity in centimeters per second squared, and z' is the thickness of the overlying rock column in centimeters. For convenience, and as an excellent approximation, the massif was divided at $z' = 6.4$ km into mafic and ultramafic levels with measured and estimated average densities of 2.9 and 3.3 g/cm³, respectively. The 0.5-kbar term is the average hydrostatic confining pressure at the top of the oceanic crust due to overlying water and sediments.

As can be seen in the table under discussion, compressional wave velocities were measured in either two or three directions at most sites, whereas shear wave velocities were commonly measured in only one. This procedure is justified among the fine-grained extrusives and sheeted dikes of the upper levels of the massif by the absence of anisotropy in V_p. For deeper levels, justification is slightly more involved. In classical seismic refraction studies at sea, only shear waves propagating in the horizontal plane with vibration confined to the vertical plane are likely to be detected. (Additional components can be detected through the use of ocean bottom seismometers, but in

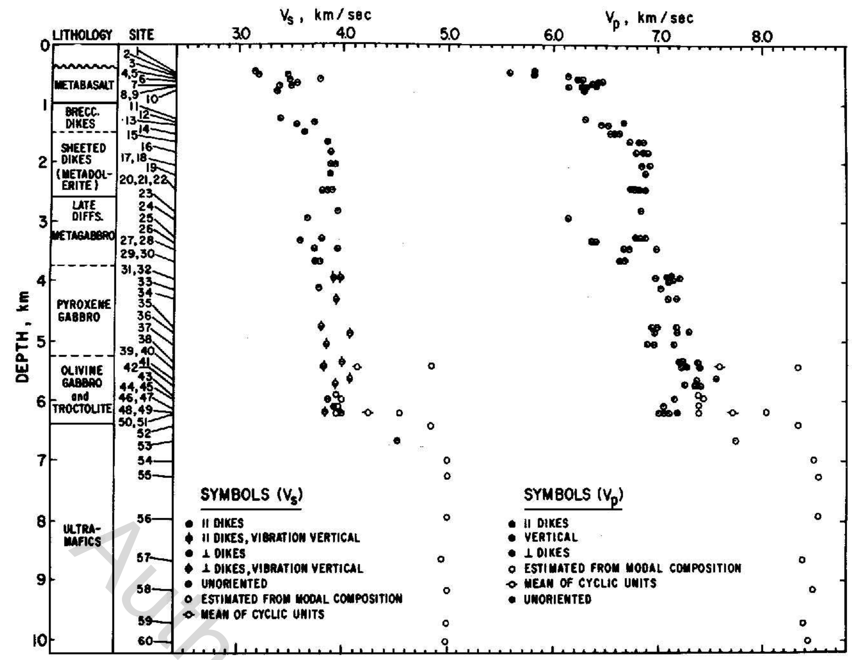

Fig. 5. Compressional (V_p) and shear (V_s) wave velocity data as a function of depth in the Blow-Me-Down massif.

practice, little of these data is yet available.) If it is proposed to compare the results of laboratory and oceanic refraction studies directly, it is only necessary to measure the velocity of shear waves propagating in the x or y directions and vibrating parallel to z. The xz or yz term following each shear velocity value in Table 1 is meant to indicate this mode of propagation, the first letter defining the propagation direction and the second the vibration direction. Where only one letter appears, the vibration direction is undefined, and where none appears, the core is unoriented. In the case of V_p, one letter suffices for an oriented core because the propagation and vibration directions are equivalent. From an examination of measured compressional wave velocities, it is apparent that samples taken from below the sheeted dikes are transversely isotropic in the horizontal plane; thus x and y are equivalent, and one core suffices.

The values of Poisson's ratio σ presented in Table 1 were computed from the relation

$$\sigma = \frac{1}{2}\left[1 - \frac{1}{(V_p/V_s)^2 - 1}\right]$$

by using the tabulated velocities for each sample. The velocities used in these computations (given in italics in Table 1) were again from cores selected to correspond in propagation direction to the propagation directions of refraction paths at sea, direct comparison of field and laboratory data thus being allowed. Though they are strictly equivalent, it should be

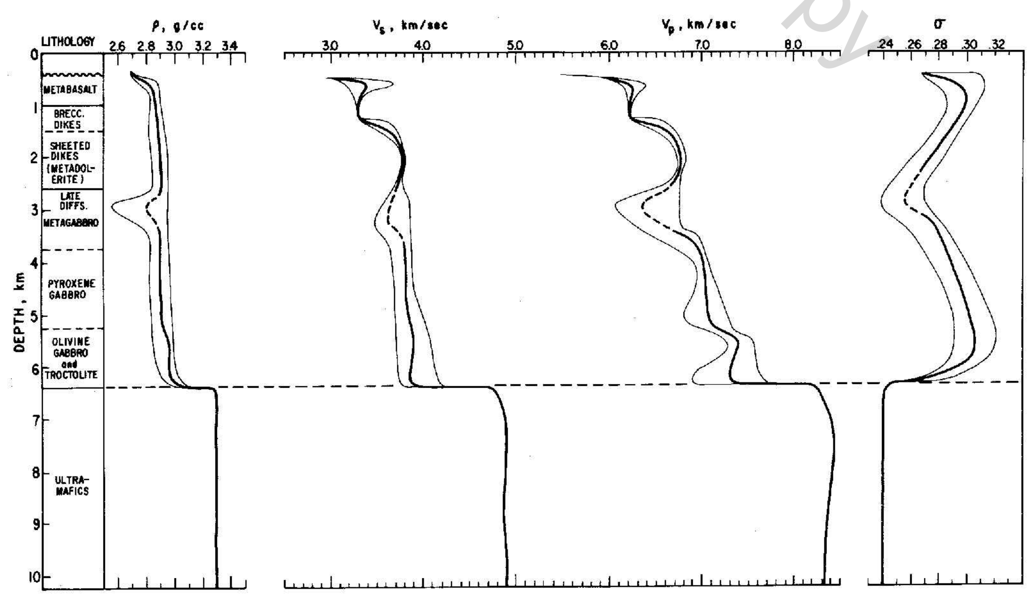

Fig. 6. Envelopes of compressional (V_p) and shear (V_s) wave velocity, density (ρ), and Poisson's ratio (σ) versus depth for the Blow-Me-Down massif. Heavy curves represent best fit to data. Dashed lines between 2.6 and 3.8 km indicate discontinuous velocity inversions. Velocities shown at depths less than 1.3 km represent maximum velocities.

noted that the values of Poisson's ratio presented here, and in all probability those determined at sea, are only apparent values, since the above equation is only rigorously correct for isotropic materials.

GEOPHYSICAL STRUCTURE OF BLOW-ME-DOWN MASSIF OF THE BAY OF ISLANDS OPHIOLITE COMPLEX

If the values of V_p and V_s given in Table 1 are plotted as a function of depth as in Figure 5 and envelopes defining the range of velocities measured in the horizontal direction are superimposed on these values, together with a best fit based upon the relative abundance of each lithology in the field as in Figure 6, the seismic velocity structure of the Blow-Me-Down massif becomes readily apparent.

The uppermost velocity unit which can be distinguished in the Blow-Me-Down massif consists of a layer approximately 1.3 km thick composed of metabasalt and the uppermost half of the brecciated dikes having measured compressional and shear wave velocities of approximately 6.20 and 3.35 km/s, respectively. The top of the unit displays a thin low-velocity cap, while toward the base, velocities again decrease slightly, giving rise to a weak velocity inversion. It should be emphasized that since laboratory measurements of velocity are made through coherent samples and do not take into account the effects of intercalated sediments, pillow interstices, and water-filled cracks and joints, all of which are common at this level, the velocities cited for this unit are maximum velocities. At greater depths, where such void space is volumetrically insignificant, its effects may be ignored.

Immediately below this unit, between depths of 1.3 and 2.6 km, is found a distinct velocity layer coincident with the lower half of the brecciated dikes and the underlying sheeted dikes. Compressional wave velocities range narrowly between 6.70 and 6.80 km/s throughout most of the layer, while shear wave velocities lie between 3.75 and 3.80 km/s. The velocity transition between this and the overlying layer, occurring almost entirely within the lower half of the brecciated dikes, is one of the sharpest in the massif.

Velocities in the metagabbros between 2.6 and 3.8 km are similar to velocities measured in the overlying sheeted dikes. The pronounced velocity inversions, particularly in V_p, at this level are associated with late differentiates and are thus laterally discontinuous, as is suggested by the dashed lines in Figure 6. Compressional and shear wave velocities thus range widely at this level between 6.0 and 6.75 km/s and 3.5 and 3.85 km/s, respectively.

The layer between 3.8 and 5.3 km, dominated by pyroxene gabbros, is characterized by a velocity gradient in which V_p and V_s slowly increase with depth from 6.9 to 7.1 and from 3.8 to 3.85 km/s, respectively. In a number of layered samples from this interval, values of V_p are observed to be fast in the vertical direction by approximately 0.1 km/s. This anisotropy is thought to originate from subparallel alignment of plagioclase long axes in the plane of layering and thus alignment of the [010] axes normal to layering; since the [010] direction in plagioclase is fast [*Alexandrov and Ryzhova,* 1962; *Ryzhova,* 1964], this would cause velocities to be high in the vertical direction. The velocity transition between this level and the overlying metagabbros varies locally between sharp and gradational extremes, depending on the presence or absence of late differentiates.

Between 5.3 and 6.4 km, in a basal velocity layer overlying the ultramafics and dominated by interlayered anorthositic olivine gabbro, troctolite, and plagioclase peridotite tectonites, V_p rises to 7.4 km/s, while V_s increases slightly to 3.9 km/s. The lower half of this level is characterized by a slight decrease in V_p and V_s to 7.3 and 3.85 km/s, respectively, giving rise to a weak, perhaps discontinuous, velocity inversion immediately overlying the ultramafics. As can be seen in Figure 5, the velocities cited for this level are based largely on reconstructed values which may be significantly in error. For purposes of reconstruction, it was assumed that (1) serpentinization is minimal at the base of the oceanic crust [e.g., *Christensen,* 1972; *Wenner and Taylor,* 1973], (2) plagioclase is similarly unaltered, (3) in situ temperature effects are minimal, and (4) the velocity of any cyclic unit is equal to the abundance-weighted mean of the velocities of its component minerals. Since serpentinization and increasing temperature lower velocity, the velocities cited may be too high. On the other hand, if olivine [010] axes are commonly vertical in the olivine-rich members of this level, as is suggested by the anisotropy of sample BOI 42, then the velocities cited may be too low.

The only anisotropy observed in the horizontal plane in the mafic levels of the massif is associated with a series of small, discontinuous bodies of foliated amphibolite found between 4.9 and 5.7 km, near the pyroxene to olivine gabbro transition. Compressional wave velocities among the amphibolites display a weak orthorhombic symmetry with V_p slow in the vertical direction and fast parallel to the lineation which is locally perpendicular to the plane of the sheeted dikes.

At 6.4 km, the boundary between the basal troctolitic olivine gabbros and the underlying ultramafics, reconstructed compressional and shear wave velocities rise to approximately 8.4 and 4.9 km/s, respectively, values maintained throughout the remaining ultramafic levels of the massif. The velocity transition, occurring in less than 50 m, is the sharpest observed in the massif.

In Figure 6, density is observed to increase slowly with depth at a rate of approximately 0.02 g/cm^3 km, from 2.85 g/cm^3 near the top of the massif to 2.98 g/cm^3 near the base of the gabbros. Below the gabbros the density of the ultramafics was assumed to be approximately 3.3 g/cm^3 (the densities of olivine, Fo_{90}, and enstatite, En_{90}, before serpentinization). The only significant departures from the mean density of 2.91 g/cm^3 observed in the mafic levels of the massif are associated with fine-grained basalts at the top of the massif, with the presence of late differentiates at a depth of 2.9 km, and with an anorthosite dike at 6.0 km.

Unlike density, Poisson's ratio σ varies markedly with depth (Figure 6). Values of σ are quite high among the extrusives near the top of the massif, ranging for the most part between 0.28 and 0.31. Within the sheeted dikes and hornblende gabbros, σ is significantly lower, ranging commonly between 0.27 and 0.29, with the late differentiates displaying values as low as 0.24. Within the pyroxene and olivine gabbros, σ increases with depth, though with considerable scatter, through ranges of 0.28–0.30 and 0.29–0.31, respectively. It should be noted that because of the presence of voids, values of σ cited for the metabasalt and brecciated dike levels of the massif represent intrinsic rather than in situ formation values.

COMPARISON WITH OCEANIC SEISMIC STRUCTURE

The velocity structure and representative values of Poisson's ratio determined above for the Blow-Me-Down massif are presented in a layered format, common to marine refraction studies, in column A of Figure 7. To compare this structure with the results of classical refraction studies, it is necessary to consider which layers would be observed and which over-

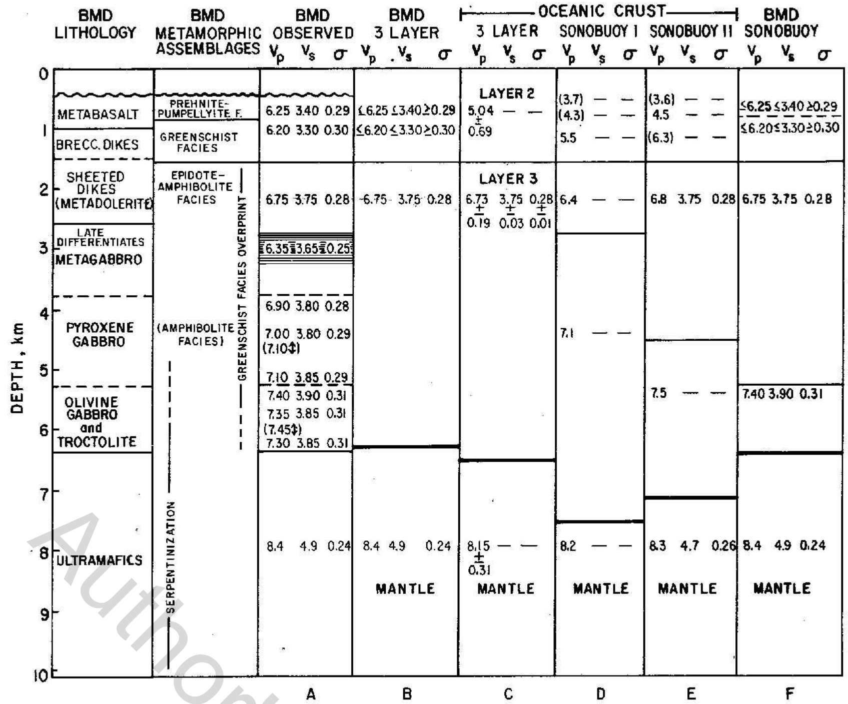

Fig. 7. Comparison of the petrology and seismic velocity structure of the Blow-Me-Down (BMD) massif with the velocity structure of the oceanic crust. Column A is the seismic velocity structure of the Blow-Me-Down massif as reconstructed in the laboratory; column B, as seen by classical refraction techniques; and column F, as seen by sonobuoy techniques. Column C is the oceanic seismic velocity structure [after *Christensen and Salisbury,* 1975] as seen by classical refraction; and columns D and E, as seen by sonobuoy techniques. The arrows after values indicate propagation velocity for vertical direction. The heavy line indicates the Mohorovičić discontinuity.

looked in a routine marine refraction survey. If the sedimentary layer, which is not exposed on the Blow-Me-Down massif, is disregarded, only three prominent basement refractors would be observed: a shallow layer between 0 and 1.3 km, a 6.75-km/s layer between 1.3 and 6.3 km, and an 8.4-km/s layer below 6.3 km.

The velocities of the uppermost refractor are somewhat uncertain because of the large gradients within this layer and the probable lowering of velocities due to voids. Thus the measured velocities presented in column B for this level represent maximum velocities. Within the 6.75-km/s layer the local velocity inversions between 2.8 and 3.3 km would be masked by the high-velocity unit at the top of the layer. Any detected change in velocity associated with the slight discontinuity at 3.8 km would either be attributed to the presence of a velocity gradient within the layer or dismissed as lying within the experimental error of the technique. The 7.40-km/s basal layer could be detected if shooting were closely spaced over the narrow interval, 25–35 km from the receiver, over which returns from this layer are observed as first arrivals. Since in practice, however, shots are often widely spaced over this interval, the 7.40-km/s layer would not commonly be observed.

Within the deepest refractor, compressional wave velocities of 8.4 km/s will be observed. As was discussed earlier in conjunction with the interpretation of reconstructed velocities, elevated temperatures may cause in situ velocities to be slightly depressed from this value.

The seismic structure outlined above is shown in column B of Figure 7 and compared with normal oceanic crustal structure as summarized by *Christensen and Salisbury* [1975] and presented in column C. It is striking that each value of velocity, Poisson's ratio, and thickness determined for the Blow-Me-Down massif of the Bay of Islands complex lies within 1 standard deviation of the corresponding independent variable defining normal oceanic structure, even where this variable is narrowly defined.

This agreement is even further emphasized if values of V_p measured through mafic samples collected from all levels of the massif are plotted as a function of V_s and σ at 1 kbar and the field of layer 3 compressional and shear wave velocities observed at sea [*Christensen and Salisbury,* 1975] is superimposed for comparison as in Figure 8. It is evident from this figure that values of V_p, V_s, and σ observed for samples from the upper levels of the intermediate refractor of the massif, that is, the metadolerites and metagabbros of the sheeted dikes, are not only central to the field of layer 3 data but uniquely coincident with its mean. It would be perverse indeed if these two refractors, indistinguishable in terms of V_p, V_s, σ, depth, and thickness, were only related by coincidence.

Recent studies using air gun sonobuoy techniques suggest that the seismic structure of the oceanic crust is far more complex than the simple three-layered model presented above [*Maynard et al.,* 1969; *Sutton et al.,* 1971; *Hussong,* 1972]. Though the results of routine refraction studies are generally consistent with those of sonobuoy studies [*Hussong,* 1972], the mean oceanic crustal layers of *Raitt* [1963] are only averages of layers which in detail are composed of several subdivisions. In particular, layer 2 is frequently observed to have a thin low-velocity cap (2.5–2.8 km/s) and layer 3 to have a thick, previously undetected basal layer with velocities ranging from 7.1 to 7.7 km/s. *Christensen and Salisbury* [1975], on the basis of sonobuoy data from main ocean basin sites for which mantle returns have been observed, identified two crustal types with distinctly different lower crustal structures. In type I of Figure 7 (column D), layer 3 is composed, on the average, of a 1-km-thick, relatively low velocity (6.4 km/s) layer underlain by a 5-km-thick layer with a velocity of 7.1 km/s. In type II (column E), on the other hand, layer 3 is composed of two subdivisions, each about 3 km thick, with velocities averaging 6.8 and 7.5 km/s.

If sonobuoy studies were conducted over the Blow-Me-Down massif in a manner analogous to that discussed above in conjunction with routine refraction studies, the velocity structure observed would be that shown in column F of Figure 7. Though similar to the three-layer structure in column B, the sonobuoy velocity column differs in two important respects. If a fractured or weathered zone is present at the top of the massif, subdivisions of the uppermost refractor could be observed, the increased structural resolution being due to the relative ease of interpreting second arrivals in such studies. In addition, the 7.40-km/s level will be detected both for this reason and because the increased shot repetition rate employed in sonobuoy studies allows first arrivals from this level to be observed routinely. The local velocity inversions between 2.8 and 3.3 km will again be masked by the overlying high-velocity level, and the discontinuity at 3.8 km will be too small to be easily detected.

A comparison of columns D and E of Figure 7 with column F illustrates the strong similarities of the Blow-Me-Down massif seismic structure with type II, the more common of the two crustal types noted from sonobuoy studies. The velocities and thicknesses of the three major refractors are in quite good agreement, as they were in the earlier three-layer comparison. In addition, the 7.4-km/s subdivision of the intermediate layer is seen to correlate with the oceanic basal layer of *Sutton et al.* [1971]. This correlation suggests, incidentally, an explanation for why shear wave velocities have proven so difficult to detect from this level even when ocean bottom seismometers are used: a 0.15-km/s shear wave velocity contrast with the overlying level would be extremely difficult to detect.

Though the conclusion that the Blow-Me-Down massif, and thus the Bay of Islands complex as a whole, is oceanic crust and the petrologic interpretations of seismic structure which follow from its acceptance seem reasonable, any test of the ophiolite hypothesis based on only one example is necessarily incomplete. Nonetheless, it is clear that at least this one ophiolite is indistinguishable from normal oceanic crust.

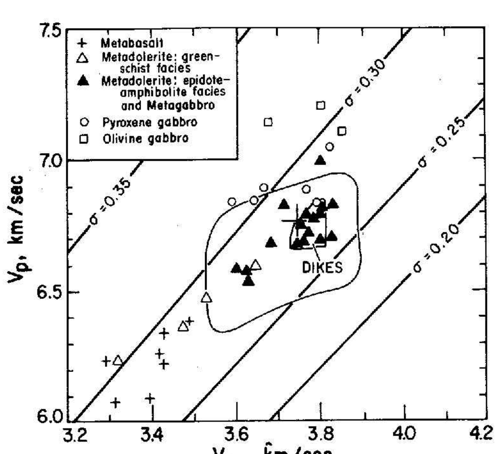

Fig. 8. Comparison of layer 3 refraction data (large enclosed field) and values of Poisson's ratio (σ), compressional wave velocity (V_p), and shear wave velocity (V_s) for mafic samples from the Blow-Me-Down massif as a function of composition. The plus sign indicates the mean of oceanic layer 3 data. Velocities reported at 1 kbar.

IMPLICATIONS AND CONCLUSIONS

If the seismic velocity structure and igneous and metamorphic petrology of the Blow-Me-Down massif traverse are presented as a function of depth as in Figure 7, it is evident that the most important factor controlling the seismic velocity structure is petrology. If the massif, and thus the Bay of Islands complex, is a segment of oceanic crust, detailed features of the seismic velocity structure of the oceanic crust can be interpreted in terms of petrology from relationships observed in the field:

1. Layer 2 is composed of fresh to slightly metamorphosed pillow and flow basalts, rubble, and intercalated sediments underlain at intermediate levels by metabasalts of the prehnite-pumpellyite facies and at deep levels by greenschist facies metabasalts and brecciated dikes. The wide range of velocities observed in layer 2 is due to variability in weathering, void space, sediments, and metamorphism.

2. At many sites in the ocean basins, the velocity discontinuity between layers 2 and 3 marks a metamorphic boundary between the greenschist and epidote-amphibolite facies, as suggested by *Christensen* [1970] from early studies of velocity through metabasalts and metagabbros. This boundary does not necessarily coincide with the boundary separating intrusive from extrusive levels of the crust; in the Blow-Me-Down massif it has penetrated to an intermediate level within the sheeted dikes coincident with the maximum depth of brecciation, suggesting that it is related to downward migration of seawater along joints and fractures.

3. Below the layer 2-3 boundary at many sites, layer 3 is composed of metadolerite sheeted dikes underlain by a thick mafic igneous intrusive complex composed of metagabbro and gabbro at high levels, fresh to weakly metamorphosed pyroxene gabbros at intermediate levels, and olivine gabbros and troctolites at the base. As can be seen in Figure 6, a pronounced velocity gradient is present in layer 3 due to increasing pyroxene and olivine content with depth, which in turn appears to be a consequence of crystal fractionation. At least locally, the intermediate, or pyroxene gabbro, level of layer 3 will be weakly anisotropic with V_p slow in the horizontal direction because of preferred orientation of plagioclase long axes parallel to cumulate layering. The high-velocity basal layer of *Sutton et al.* [1971] is coincident with the level at the base of the sequence composed of strongly banded olivine gabbro and troctolite tectonites.

4. The 7.1-km/s layer observed in the crustal type I of *Christensen and Salisbury* [1975] appears to be composed of pyroxene gabbro mixed, perhaps, with small amounts of olivine gabbro. This lithology is observed at intermediate levels in the Blow-Me-Down massif but is masked as a refractor by the overlying 6.75-km/s level. It is intriguing to speculate that the velocity column of the massif and of crustal type II could evolve to that of type I simply by downward migration of seawater and the metamorphic boundary separating layers 2 and 3. As the boundary moves downward leaving low-velocity greenschist facies metadolerites in its wake, the metagabbro level would thin and eventually become seismically undetectable. As the sheeted dikes decreased in velocity to transitional values of 6.4 km/s, the underlying pyroxene gabbro level would become a distinct refractor in response to the increase in velocity contrast between levels. The 7.4-km/s level, on the other hand, would become masked.

This scenario suggests that crustal type I may be more common in old crust.

5. Two velocity inversions will commonly be present in the oceanic crust, one at the base of layer 2 caused by the presence of high-velocity prehnite-pumpellyite facies metabasalts overlying low-velocity greenschist facies metabasalts and metadolerites and a second at intermediate levels in layer 3 caused by the presence of low-velocity quartz-rich late differentiates below the sheeted dikes. Both inversions will tend to be discontinuous in nature, the former because of lateral variations in void space, weathering, and metamorphism in layer 2 and the latter because the late differentiates are only present in the crust as small pods and intrusions and are thus of limited lateral extent. The inversion associated with late differentiates is distinctive in that it is much more strongly developed in V_p than in V_s. Values of V_p/V_s and Poisson's ratio σ will thus be low wherever such an inversion is developed.

6. The Mohorovičić discontinuity represents a transition from rocks of gabbroic to ultramafic composition caused initially, perhaps, by the first appearance of plagioclase as a cumulus phase during crystal fractionation. Disseminated plagioclase is present in the ultramafics below the discontinuity [e.g., *Smith,* 1958; *Moores and Vine,* 1971; *Moores and Jackson,* 1974] but not in sufficient quantity to lower velocities below those characteristic of the oceanic mantle.

Finally, it should be noted that the petrologic and seismic velocity structures indicated above for the oceanic crust are, in fact, logical consequences of igneous and metamorphic processes long thought to operate in the sea floor. Although it must be recalled that the conclusions reached here have been drawn from the study of only one traverse across one ophiolite complex among many, the overall similarity of the ophiolites, the remarkable agreement between the seismic velocity structure of the Blow-Me-Down massif of the Bay of Islands complex and that of the oceanic crust, and the overall uniformity of oceanic seismic structure all argue for their general validity. It is thus concluded on the basis of geophysical evidence that the ophiolites, and in particular, the Bay of Islands complex, are segments of oceanic crust emplaced on land and that their examination not only allows a direct interpretation of oceanic seismic structure in terms of petrology but also provides an understanding of the processes which predominate in the formation and evolution of the oceanic crust.

Acknowledgments. We are indebted to many for assistance in this study, especially to D. Borns, M. Brown, D. Fountain, P. Hoddinott, and R. McConaghy. We also wish to thank H. Williams for his excellent advice during the planning of this investigation. Financial support was provided by Office of Naval Research contract N-00014-75-C-0502 and Geological Society of America grant 1680-73.

REFERENCES

Alexandrov, K. S., and T. V. Ryzhova, Elastic properties of rock-forming minerals, 3, Feldspars, *Izv. Acad. Sci. USSR Phys. Solid Earth, 2,* 129–131, 1962.

Birch, F., The velocity of compressional waves in rocks to 10 kilobars, 1, *J. Geophys. Res., 65,* 1083–1102, 1960.

Buddington, A. F., and H. H. Hess, Layered peridotite laccoliths in the Trout River area, Newfoundland, *Amer. J. Sci., 33,* 380–388, 1937.

Christensen, N. I., Shear wave velocities in metamorphic rocks at pressures to 10 kilobars, *J. Geophys. Res., 71,* 3549–3556, 1966.

Christensen, N. I., Composition and evolution of the oceanic crust, *Mar. Geol., 8,* 139–154, 1970.

Christensen, N. I., The abundance of serpentinites in the ocean crust, *J. Geol., 80,* 709–719, 1972.

Christensen, N. I., Seismic structure of the oceanic lithosphere as determined from seismic velocities in West Coast ophiolites (abstract), *Eos Trans. AGU, 56*(12), 1079, 1975.

Christensen, N. I., and M. H. Salisbury, Sea floor spreading, progressive alteration of layer 2 basalts, and associated changes in seismic velocities, *Earth Planet. Sci. Lett., 15,* 367–375, 1972.

Christensen, N. I., and M. H. Salisbury, Velocities, elastic moduli and weathering-age relations for Pacific layer 2 basalts, *Earth Planet. Sci. Lett., 19,* 461–470, 1973.

Christensen, N. I., and M. H. Salisbury, Structure and constitution of the lower oceanic crust, *Rev. Geophys. Space Phys., 13,* 57–86, 1975.

Christensen, N. I., and G. H. Shaw, Elasticity of mafic rocks from the mid-Atlantic ridge, *Geophys. J. Roy. Astron. Soc., 20,* 271–284, 1970.

Church, W. R., and R. K. Stevens, Early Paleozoic ophiolite complexes of the Newfoundland Appalachians as mantle-oceanic crust sequences, *J. Geophys. Res., 76,* 1460–1466, 1971.

Davies, H. L., Peridotite-gabbro-basalt complex in eastern Papua: An overthrust plate of oceanic mantle and crust, *Bull. Bur. Miner. Resour. Geol. Geophys. Aust., 128,* 47 pp., 1971.

Dewey, J. F., P. J. Fox, and W. S. F. Kidd, Structure and generation of oceanic crust and mantle (abstract), *Geol. Soc. Amer. Abstr. Programs, 5,* 597–598, 1973.

Dortman, N. B., and M. Sh. Magid, New data on velocity of elastic waves in crystalline rocks as a function of moisture, *Int. Geol. Rev., 11,* 517–523, 1969.

Engel, C. G., and R. L. Fisher, Lherzolite, anorthosite, gabbro and basalt dredged from the mid-Indian Ocean ridge, *Science, 166,* 1136–1141, 1969.

Fox, P. J., E. Schreiber, and J. J. Peterson, The geology of the oceanic crust: Compressional wave velocities of oceanic rocks, *J. Geophys. Res., 78,* 5155–5172, 1973.

Gass, I. G., and D. Masson-Smith, The geology and gravity anomalies of the Troodos massif, Cyprus, *Phil. Trans. Roy. Soc. London, Ser. A, 255,* 417–467, 1963.

Gass, I. G., and J. D. Smewing, Intrusion, extrusion and metamorphism at constructive margins: Evidence from the Troodos massif, Cyprus, *Nature, 242,* 26–29, 1973.

Hussong, D. M., Detailed structural interpretations of the Pacific oceanic crust using Asper and ocean bottom seismometer methods, Ph.D. thesis, 165 pp., Univ. of Hawaii, Honolulu, 1972.

Lort, J. M., and D. H. Matthews, Seismic velocities measured in rocks of the Troodos igneous complex, *Geophys. J. Roy. Astron. Soc., 27,* 383–392, 1972.

Matthews, D. H., J. Lort, T. Vertue, C. K. Poster, and I. G. Gass, Seismic velocities at the Troodos outcrop, *Nature Phys. Sci., 231,* 200–201, 1971.

Maynard, G. L., G. H. Sutton, and D. M. Hussong, Seismic observations in the Solomon Islands and Darwin Rise regions using repetitive sources (abstract), *Eos Trans. AGU, 50*(4), 206, 1969.

Miyashiro, A., F. Shido, and M. Ewing, Metamorphism in the mid-Atlantic ridge near 24° and 30°N, *Phil. Trans. Roy. Soc. London, Ser. A, 268,* 589–603, 1971.

Moores, E. M., and E. D. Jackson, Ophiolites and oceanic crust, *Nature, 250,* 136–138, 1974.

Moores, E. M., and F. J. Vine, The Troodos massif, Cyprus, and other ophiolites as oceanic crust: Evaluation and implications, *Phil. Trans. Roy. Soc. London, Ser. A, 268,* 443–466, 1971.

Nur, A., and G. Simmons, The effect of saturation on velocity in low porosity rocks, *Earth Planet. Sci. Lett., 7,* 183–193, 1969.

Peterson, J. J., P. J. Fox, and E. Schreiber, Newfoundland ophiolites and the geology of the oceanic layer, *Nature, 247,* 194–196, 1974.

Poster, C. K., Ultrasonic velocities in rocks from the Troodos massif, Cyprus, *Nature Phys. Sci., 243,* 2–3, 1973.

Raitt, R. W., The crustal rocks, in *The Sea,* vol. 3, edited by M. N. Hill, pp. 85–102, John Wiley, New York, 1963.

Ryzhova, T. V., Elastic properties of plagioclase, *Izv. Acad. Sci. USSR Phys. Solid Earth, 7,* 633–635, 1964.

Smith, C. H., Bay of Islands igneous complex, western Newfoundland, *Geol. Surv. Can. Mem., 290,* 132 pp., 1958.

Sutton, G. H., G. L. Maynard, and D. M. Hussong, Widespread occurrence of a high-velocity basal layer in the Pacific crust found with repetitive sources and sonobuoys, in *The Structure and Physical Properties of the Earth's Crust, Geophys. Monogr. Ser.,* vol. 14, edited by J. G. Heacock, pp. 193–209, AGU, Washington, D. C., 1971.

Varne, R., and M. J. Rubenach, Geology of Macquarie Island and its relationship to oceanic crust, in *Antarctic Oceanology II: The Australian-New Zealand Sector, Antarctic Res. Ser.,* vol. 19, edited by D. E. Hayes, pp. 251–266, AGU, Washington, D. C., 1972.

Wenner, D. B., and H. P. Taylor, Jr., Oxygen and hydrogen isotope studies of the serpentinization of ultramafic rocks in oceanic envi-

ronments and continental ophiolite complexes, *Amer. J. Sci., 273*, 207–239, 1973.
Williams, H., Mafic-ultramafic complexes in western Newfoundland Appalachians and the evidence for transportation: A review and interim report, *Proc. Geol. Ass. Can., 24*(1), 9–25, 1971.
Williams, H., The Bay of Islands map area, Newfoundland, *Geol. Surv. Can. Pap., 72-34*, 1–7, 1973.
Williams, H., and J. Malpas, Sheeted dikes and brecciated dike rocks within transported igneous complexes, Bay of Islands, western Newfoundland, *Can. J. Earth Sci., 9*, 1216–1229, 1972.
Williams, H., and W. K. Smyth, Metamorphic aureoles beneath ophiolite suites and alpine peridotites: Tectonic implications with west Newfoundland examples, *Amer. J. Sci., 273*, 594–621, 1973.
Williams, H., M. J. Kennedy, and E. R. W. Neale, The Appalachian Structural Province, Structural Styles in Canada, *Geol. Ass. Can. Spec. Pap., 11*, 181–261, 1972.

(Received November 22, 1976;
revised October 11, 1977;
accepted October 21, 1977.)